

# Correlation of Water Vapor Adsorption Behavior of Wood with Surface Thermodynamic Properties

MANDLA A. TSHABALALA,<sup>1</sup> AGNES R. DENES,<sup>2</sup> R. SAM WILLIAMS<sup>1</sup>

<sup>1</sup> U.S. Department of Agriculture, Forest Service, Forest Products Laboratory, One Gifford Pinchot Drive, Madison, Wisconsin 53705-2398

<sup>2</sup> Engineering Research Center for Plasma-Aided Manufacturing, University of Wisconsin, Madison, Wisconsin 53705

Received 28 May 1998; accepted 10 November 1998

**ABSTRACT:** To improve the overall performance of wood-plastic composites, appropriate technologies are needed to control moisture sorption and to improve the interaction of wood fiber with selected hydrophobic matrices. The objective of this study was to determine the surface thermodynamic characteristics of a wood fiber and to correlate those characteristics with the fiber's water vapor adsorption behavior. The surface thermodynamic properties, determined by inverse gas chromatography at infinite dilution or near zero surface coverage, were the dispersive component of the surface energy, surface acid-base free energy and enthalpy of desorption of acid-base probes, and surface acid-base acceptor and donor parameters ( $K_A$  and  $K_D$ ). Water vapor adsorption was expressed in terms of the percentage of weight gain ( $\Delta W\%$ ) resulting from water vapor adsorption on the wood particles, calculated relative to their initial weight after preconditioning in a vacuum desiccator at room temperature. The results showed a strong correlation between  $\Delta W\%$  and  $K_A$ , and between  $\Delta W\%$  and surface acid-base free energy of water desorption ( $\Delta H_{\text{water}}^{\text{AB}}$ ), calculated from experimental  $K_A$  and  $K_D$  and values in the literature for acceptor and donor values of water. These results suggest that for substrates such as wood, whose surface Lewis acid-base properties are characterized by a relatively stronger tendency to accept electrons, the key to controlling water vapor adsorption is to manipulate the magnitude of  $\Delta H_{\text{water}}^{\text{AB}}$ , primarily via  $K_A$ , and to a lesser extent via  $K_D$ . © 1999 John Wiley & Sons, Inc. \* J Appl Polym Sci 73: 399-407, 1999

**Key words:** wood particles; water vapor adsorption; surface acid-base enthalpy; inverse gas chromatography; acceptor and donor parameters

## INTRODUCTION

Agricultural resources, including forest products, constitute the most abundant renewable resources worldwide. Recently, renewed interest has been expressed in using these resources to

develop environmentally friendly composite materials for new and existing applications. Much research effort has focused on using these resources as fillers in such relatively low-cost matrices as polyethylene, polypropylene, polystyrene, and polyester.<sup>1-4</sup> Researchers have observed that although wood-plastic composites generally exhibit lower mechanical properties compared to composites made with glass, carbon, or aramid plastic, they, nonetheless, offer several attractive features. Wood-plastic composites have a comparatively superior performance-to-

---

Correspondence to: M. A. Tshabalala.

Contract grant sponsor: The USDA Forest Service.

Journal of Applied Polymer Science, Vol. 73, 399-407 (1999)

© 1999 John Wiley & Sons, Inc. \* This article is a US Government work and, as such, is in the public domain in the United States of America.

CCC 0021-8995/99/030399-09

by biodegradation or incineration without releasing noxious gases.<sup>5</sup>

A number of fundamental issues remain to be resolved to improve the overall performance of wood-plastic composites. Two issues are developing appropriate technologies for controlling moisture sorption and improving the interaction of wood fiber with selected hydrophobic matrices. The objective of the study reported here was to determine the surface thermodynamic characteristics of a wood fiber and to correlate those characteristics with water vapor adsorption behavior of the fiber. Such information is relevant to the design of appropriate processes for manipulating the surface properties of wood fibers while preserving their desirable bulk properties. A desirable property for wood-plastic composites is optimal adhesion to nonwood matrices, and for fiberboard, particleboard, and flakeboard, resistance to degradation mediated by water vapor adsorption.

## BACKGROUND

All three major components of the wood cell wall—cellulose, hemicellulose, and lignin—contain atomic sites that are capable of donating or accepting electrons. In the case of cellulose and hemicelluloses, the most likely electron donors are the oxygen atoms, and the hydrogen atoms in the hydroxyl groups act as electron acceptors. In the case of lignin, the most likely electron-donor sites are the phenyl rings and the oxygen atoms, and the hydrogen atoms in the hydroxyl groups are likely to be electron acceptor sites. Because water also contains both electron donor and acceptor sites, it has the capacity to interact with components of the wood cell wall by an electron acceptor-donor mechanism. These interactions are commonly referred to as hydrogen-bonding reactions, and they constitute a subset of Lewis acid-base interactions.<sup>6</sup>

The Lewis acid-base properties of many liquids, including water, have been quantitatively characterized by acceptor and donor numbers, AN and DN, respectively.<sup>7,8</sup> By analogy, the Lewis acid-base properties of solid surfaces can be quantitatively characterized by acceptor and donor parameters,  $K_A$  and  $K_D$ , respectively.<sup>9,10</sup> Thus, if  $K_A$  and  $K_D$  of wood particle surfaces and the literature values for AN and DN are known, it should be possible to use Papirer's approach<sup>11</sup> to calculate the surface acid-base enthalpy of interaction of wood particles with water vapor and to determine the effect of different

surface treatments or modifications on the magnitude of this parameter.

The conventional methods for determining the surface thermodynamic parameters of wood fiber are based on calorimetry<sup>12</sup> and contact angle analysis.<sup>13,14</sup> Calorimetric methods yield a thermodynamic quantity, called the heat of wetting, from which the differential heats of sorption can be calculated. Contact angle analysis methods have been applied successfully to determine dispersive and polar components of surface energy. However, these methods are generally suitable for application to materials with smooth nonporous surfaces. For materials with rough porous surfaces, like wood, an alternative method based on inverse gas chromatography has been found to be more suitable.<sup>15,16</sup> Inverse gas chromatography (IGC) consists of measuring the chromatographic retention times of vapor-phase probes of known thermodynamic properties on a column packed with the material of interest. Saturated *n*-alkane probes are used to estimate the dispersive component of the surface energy, and acid-base probes are used to estimate the Lewis acid-base characteristics of the substrate of interest.

In the present study, ICC at infinite dilution or near-zero surface coverage was used to estimate the dispersive component of the surface energy ( $\gamma_S^D$ ), the surface acid-base free energy of desorption ( $\Delta G^{AB}$ ), and enthalpy of desorption ( $\Delta H^{AB}$ ) of acid-base probes, and the surface acceptor and donor parameters ( $K_A$  and  $K_D$ ) of wood particles. The  $K_A$  and  $K_D$  values were used to calculate the surface acid-base enthalpy of water desorption ( $\Delta H_{\text{water}}^{AB}$ ).

The degree of correlation between the  $\Delta W\%$  values for the three kinds of particles (Fig. 1), and the calculated thermodynamic values,  $K_A$ ,  $K_D$ ,  $\Delta H_{\text{water}}^{AB}$  (Table III), and  $\gamma_S^D$  at 27°C (Table VI) was determined by means of the Excel Analysis Toolpak. The output was a symmetrical matrix of correlation coefficients. For the correlation to be considered significant, the value of the correlation coefficient between the independent variables,  $\Delta W\%$ , and  $K_A$ ,  $K_D$ ,  $\Delta H_{\text{water}}^{AB}$ , and  $\gamma_S^D$  must be close to unity.

## EXPERIMENTAL

### Materials

Loblolly pine (*Pinus taeda* L.) was ground into particles in a Wiley mill. The ground wood was

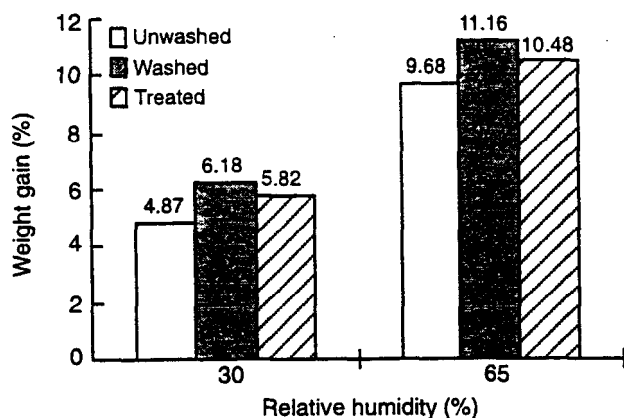


**Figure 1** Weight percent gain of wood particles conditioned at 30 or 65% relative humidity.

passed through a set of sieves, and the 60/80 mesh fraction was used in this study. Particles subjected to only this procedure will be referred to as unwashed.

Washed wood particles were prepared from unwashed particles by successive 24-h extractions with toluene/ethanol (2/1 v/v) followed by ethanol in a Soxhlet apparatus and with boiling water in an Erlenmeyer flask for approximately 1 h. The washed wood particles were air dried and stored in sealed glass jars. The average weight percent loss after washing and air drying was  $12.0 \pm 2.0$  percent ( $n = 5$ ), which reflected the total weight loss due to a combination of losses from washing, filtration, transfer, and other related sample manipulation procedures.

Treated wood particles were prepared by exposing the washed wood particles for 15 min to a cold plasma sustained in hexamethyldisiloxane (HMDSO) vapor.<sup>18,19</sup> The treatment was performed in an experimental capacitance coupled rotary reactor equipped with a radio frequency (13.56 MHz) power generator. The sample was loaded into the reaction chamber, and the chamber was evacuated to a base pressure of 0.02 mmHg. The HMDSO vapor stored in the reservoir was bled into the reactor, and the plasma was initiated at a power of 200 W. The pressure in the chamber during the reaction was 0.3 mmHg. The treated wood particles were stored in sealed plastic bags. The percent weight uptake from cold plasma treatment was not determined because it was masked by losses arising from transfer of the treated particles from the cold plasma reactor.

The HPLC-grade solvents (hexane, heptane, octane, nonane, decane, carbon tetrachloride,

chloroform, diethyl ether, and ethyl acetate) used as IGC probes, methane gas (1000 ppm in nitrogen) used as the IGC marker, and HMDSO were all purchased from Sigma-Aldrich (Milwaukee, WI). (The use of trade or firm names in this publication is for reader information, and does not imply endorsement by the U.S. Department of Agriculture of any product or service.)

#### Water Vapor Adsorption Measurements

Approximately 1-g samples of wood particles in separate aluminum foil dishes were placed in a vacuum desiccator at room temperature and conditioned for 72 h. The samples were weighed accurately to 0.0001 g before being placed in an open box for conditioning in environmental chambers to a dry-bulb temperature of 27°C and 30 or 65% relative humidity. A constant weight was attained within 1 day. The samples were left in the environmental chamber for an additional 9 days, during which period they were weighed daily. The percentage of weight gain ( $\Delta W\%$ ) resulting from water vapor adsorption was calculated on the basis of the weight of the sample preconditioned in a vacuum desiccator at room temperature for a minimum of 72 h.

#### IGC Measurements

A gas chromatograph equipped with a flame ionization detector was used for IGC measurements. The samples were packed under vacuum in a deactivated glass column 1.2 m long with a 4-mm internal diameter (Alltech Associates, Deerfield, IL). The deactivated glass column was rinsed with acetone and methanol, and dried under nitrogen flow in the GC oven at 40°C before it was packed with a sample of the wood particles. The average weight of the wood particles in the column was  $4.1 \pm 0.1$  g ( $n = 6$ ). Saturated *n*-alkanes were used as the neutral probes, and carbon tetrachloride, chloroform, diethyl ether, and ethyl acetate were used as the acid-base probes. The specific retention volume for each probe was determined from the average of quadruplicate measurements of the corresponding retention time. Detailed procedures for performing IGC measurements and for treatment of the data were described previously.<sup>16</sup> In summary, under conditions of near-zero surface coverage, the specific retention volume  $V_g$ , defined as the volume of carrier gas per gram of test material required to elute a probe from the column, can be related to

various surface thermodynamic parameters. Thus, the dispersive component of the surface energy of wood particles,  $\gamma_S^D$ , is related to  $V_g$  by the following equation:

$$RT \ln V_g = 2N(\gamma_S^D)^{1/2} a(\gamma_L^D)^{1/2} + C \quad (1)$$

where  $R$  is the gas constant,  $T$  is the column absolute temperature,  $N$  is Avogadro's number,  $a$  is the surface area of the probe molecule,  $\gamma_L^D$  is the dispersive component of the surface energy of the probe in the liquid state, and  $C$  is a constant. A plot of  $RT \ln V_g$  versus  $2Na(\gamma_L^D)^{1/2}$  should give a straight line with slope  $(\gamma_S^D)^{1/2}$ .

The acid-base enthalpy of desorption,  $\Delta H^{AB}$ , was calculated from the acid-base free energy of desorption,  $\Delta G^{AB}$ , which is related to the specific retention volume of the acid-base probe by the following equation:

$$RT \ln(V_g/V_g^{\text{ref}}) = \Delta G^{AB} \quad (2)$$

where  $V_g$  is the specific retention volume of the acid-base probe, and  $V_g^{\text{ref}}$  is the specific retention volume of an hypothetical alkane with the same  $a(\gamma_L^D)^{1/2}$  as that of the polar probe.

$\Delta G^{AB}$  is related to  $\Delta H^{AB}$  by the following equation:

$$\Delta G^{AB} = \Delta H^{AB} - T\Delta S^{AB} \quad (3)$$

where  $\Delta S^{AB}$  is the entropy of desorption of the acid-base probe. Thus, a plot of  $\Delta G^{AB}/T$  versus  $1/T$  should yield a straight line with slope  $\Delta H^{AB}$ .

The surface acceptor ( $K_A$ ) and donor ( $K_D$ ) parameters are related to  $\Delta H^{AB}$  by the following equation:

$$\Delta H^{AB} = K_A DN + K_D AN \quad (4)$$

where  $DN$  and  $AN$  are the respective literature donor and acceptor numbers of the acid-base probe.<sup>7</sup> A plot of  $\Delta H^{AB}/AN$  versus  $DN/AN$  should yield a straight line with slope  $K_A$  and intercept  $KD$ .

The acid-base enthalpy of desorption of water from the wood particles was calculated from the following relationship:

$$\Delta H_{\text{water}}^{AB} = (18K_A + 54.8K_D)4.18 \quad (5)$$

where 18 is kcal/mol and 54.8, a dimensionless quantity, are the respective literature values of the donor and acceptor numbers for water.<sup>7,8</sup>

## Other Measurements

The surface chemistry of the wood particles was elaborated by X-ray photoelectron spectroscopy (XPS) and by energy-dispersive X-ray analysis (EDXA).

To elucidate the nature of the interaction of the HMDSO plasma products with the surface of the wood particles, the treated particles were extracted for 24 h with acetone in a Soxhlet apparatus. The extracted particles were analyzed for silicon by EDXA. The acetone extract was evaporated in a vial to near dryness at room temperature under a gentle stream of nitrogen. The residual film in the vial was reconstituted in chloroform and analyzed by Fourier Transform infrared (FTIR), and carbon-13 and proton nuclear magnetic resonance (NMR) spectroscopy.

## RESULTS AND DISCUSSION

### Water Vapor Adsorption

The percentage of weight gain ( $\Delta W\%$ ) of wood particles conditioned at 30 or 65% relative humidity at a constant temperature of 27°C is shown in Figure 1. The washed wood particles adsorbed the greatest amount of water vapor, and the unwashed wood particles, the least. Water vapor adsorption of the HMDSO-treated wood particles was intermediate that of the washed and unwashed particles. This result was not surprising, because we expected that the removal of extractives would expose more hydrophilic sites per unit weight of the wood particles, while the deposition of cold plasma products of HMDSO on the surface of the particles would modify their water vapor adsorption behavior. However, contrary to expectations, HMDSO treatment, under the conditions described for the present study, did not mitigate the water vapor adsorption behavior of the washed particles to the same extent as that demonstrated by the native unwashed particles.

### Surface Chemistry of HMDSO Plasma-Treated Wood Particles

As shown in Figure 2, there was no significant difference between the EDXA spectra of HMDSO-treated wood particles before [Fig. 2(B)] and after

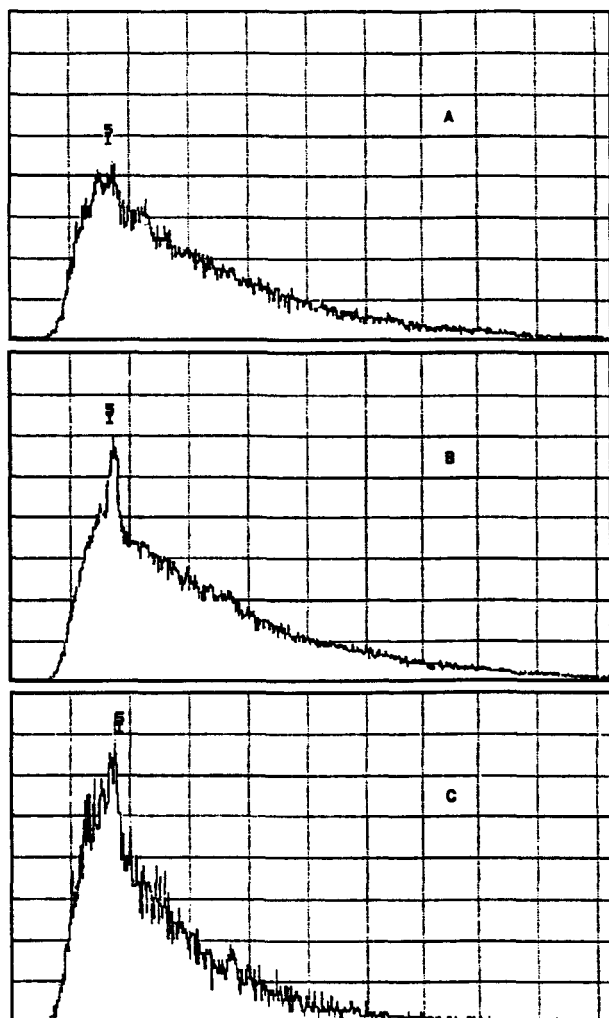


**Figure 2** EDXA spectra of (A) control and HMDSO plasma-treated wood particles, (B) before, and (C) after 24-h Soxhlet extraction with acetone.

[Fig. 2(C)] a 24-h Soxhlet extraction with acetone. In addition, the FTIR spectra of the acetone extracts of HMDSO-treated particles did not show any presence of HMDSO or silicon containing structures. However, the carbon-13 and proton NMR spectra of the extracts, in deuterated chloroform, showed a structure with methyl groups attached to a silicon atom. These results suggest that HMDSO plasma deposits on the wood particles may consist of multiple layers, with the first layer being chemically bound to the wood substrate, and the subsequent layers growing on the first layer by crosslinking mechanisms. The methyl-silicon structure observed in the NMR spectra may have derived from the nonchemically bound layers of the thin film deposits.

Previous studies on the chemistry of the HMDSO cold plasma products have proposed the presence of trimethyl silyl and penta-methyl disiloxane species shown in Figure 3(A).<sup>20</sup> Such species could conceivably react with labile surface hydroxyl groups on the wood substrate according to the scheme shown in Figure 3(B).

#### Plots of $\Delta G^{A/B}/T$ Versus $1/T$

Table I shows the surface acid-base free energy of desorption ( $\Delta G^{AB}$ ) values of IGC probes for wood particles calculated according to eq. (2). These values were used to generate the plots of  $\Delta G^{A/B}/T$  as a function of  $1/T$  (Figs. 4-6), from which the  $\Delta H^{AB}$  values for unwashed, washed, and treated wood particles were determined. Plots of the data for unwashed particles resulted in straight lines that were almost parallel to the horizontal axis, indicating relatively weak surface acid-base characteristics (Fig. 4). By contrast, plots of the data for washed (Fig. 5) and treated (Fig. 6) particles resulted in straight lines with well-defined slopes, indicating relatively strong surface acid-base characteristics.

#### Plots of $\Delta H^{AB}$ Versus DN/AN

Table II shows  $\Delta H^{AB}$  values of IGC probes for wood particles calculated according to eq. (3). These values were used to generate the plots of

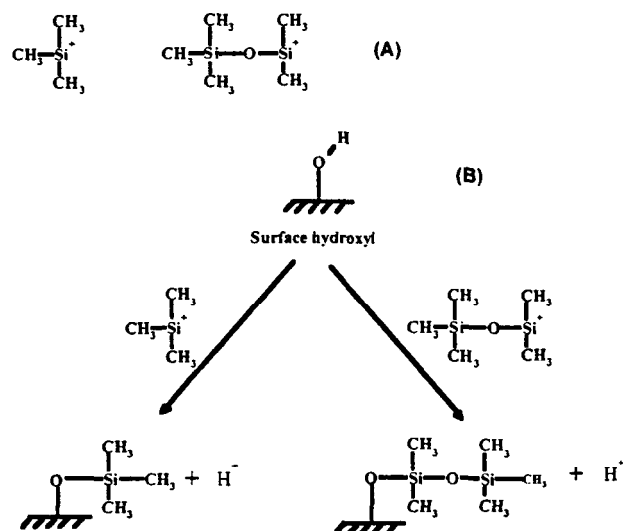


**Figure 3** (A) Some suggested possible structures in a cold HMDSO plasma (from ref. 20), and (B) proposed possible reaction pathway of HMDSO plasma products with a wood substrate.

**Table I** Surface Acid-Base Free Energy of Desorption ( $\Delta G^{AB}$ ) of Acid-Base Probes on Wood Particles

Substrate and Probe	$\Delta G^{AB}$ (kJ/mol) at Various Temperatures				
	40°C	50°C	60°C	80°C	100°C
Unwashed particles					
CCl <sub>4</sub>	1.64	1.79	1.89	2.51	1.92
CHCl <sub>3</sub>	4.12	4.14	4.08	4.71	3.77
C <sub>2</sub> H <sub>5</sub> OC <sub>2</sub> H <sub>5</sub>	2.03	2.14	2.54	2.30	2.28
CH <sub>3</sub> COOC <sub>2</sub> H <sub>5</sub>	5.35	5.41	5.09	5.52	4.47
Washed particles					
CCl <sub>4</sub>	-0.62	-0.55	-0.59	-0.25	-0.78
CHCl <sub>3</sub>	3.03	2.80	2.67	2.58	2.32
C <sub>2</sub> H <sub>5</sub> OC <sub>2</sub> H <sub>5</sub>	5.28	4.76	4.44	3.97	2.97
CH <sub>3</sub> COOC <sub>2</sub> H <sub>5</sub>	9.78	9.18	8.74	7.97	6.92
Treated particles					
CCl <sub>4</sub>	0.28	0.22	0.08	0.02	0.59
CHCl <sub>3</sub>	4.34	3.99	3.64	3.33	3.68
C <sub>2</sub> H <sub>5</sub> OC <sub>2</sub> H <sub>5</sub>	4.90	4.38	3.68	2.81	4.27
CH <sub>3</sub> COOC <sub>2</sub> H <sub>5</sub>	10.23	9.74	9.03	7.75	8.65

$\Delta H^{AB}/AN$  versus  $DN/AN$  (Fig. 7), from which the values of  $K_A$  and  $K_D$  were estimated according to eq. (4). As shown in Figure 7, the  $\Delta H^{AB}/AN$  versus  $DN/AN$  plots for washed and treated particles were nearly straight lines with well-defined slopes. As expected, the plot for the unwashed particles resulted in a nearly straight line that was almost parallel to the horizontal axis, with a slope that was negligible or nearly equal to zero, for all practical purposes. As stated in the Background, the latter result is consistent with a surface that has very few or no Lewis acid-base characteristics.

#### Interaction with Water Vapor

The experimental values of  $K_A$  and  $K_D$ , used to calculate the values of  $\Delta H^{AB}_{water}$  for unwashed,

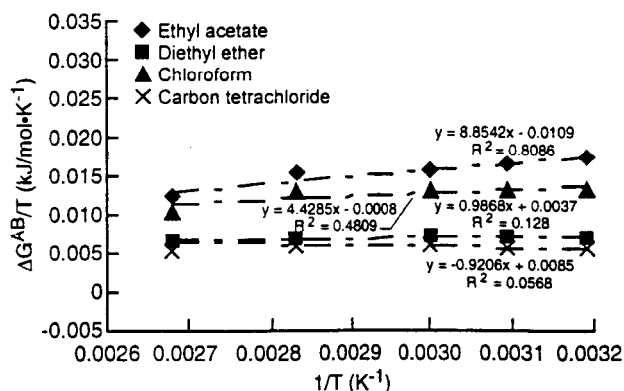


**Figure 4**  $\Delta G^{AB}/T$  as a function of  $1/T$  for unwashed wood particles.

washed, and treated wood particles according to eq. (5), are listed in Table III. Contrary to expectations, there was no significant difference between the values for the washed and treated wood particles. The HMDSO plasma had apparently little or no effect on wood particle surface, or possibly the treatment led to the formation of new oxygenated carbon species at the expense of the hydrogen and carbon composition of the surface, as supported by the high resolution X-ray photoelectron spectral data in Table IV. These data show the presence of a spurious carbonate-like structure on the surface of the treated wood particles that was not detected on the washed wood particles. The origin of this carbonate-like structure is unknown.

The objective of the present study was to investigate the role of the surface thermodynamic

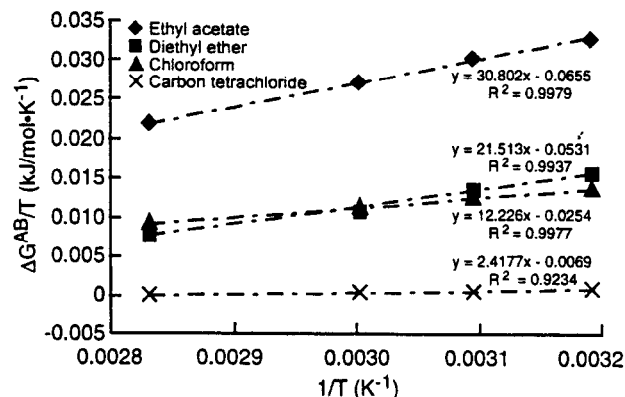


**Figure 5**  $\Delta G^{AB}/T$  as a function of  $1/T$  for washed wood particles.

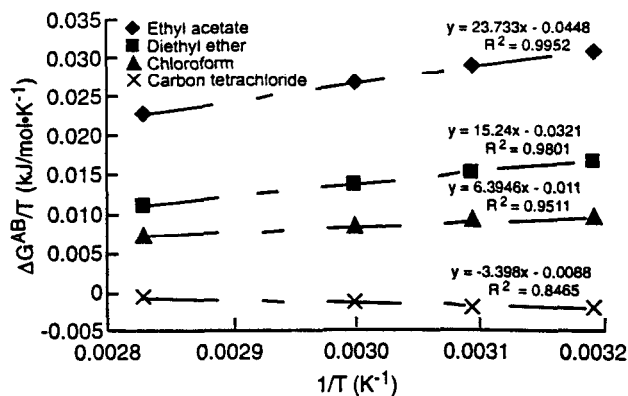


**Figure 6**  $\Delta G^{A B}/T$  as a function of  $1/T$  for treated wood particles.

properties of unwashed, washed, and HMDSO-treated wood particles in water vapor adsorption. This was accomplished by statistical correlation of the percentage of weight gain ( $\Delta W\%$ ) of the particles caused by water vapor adsorption at different relative humidity levels with the surface thermodynamic parameters  $\Delta H_{\text{water}}^{\text{AB}}$ ,  $K_A$ ,  $K_D$ , and  $\gamma_S^D$ . As shown in Table V, there was a strong correlation between  $\Delta W\%$  and  $\Delta H_{\text{water}}^{\text{AB}}$  at 30% RH only, and between  $\Delta W\%$  and  $K_A$  at 30 and 65% RH. However,  $\Delta W\%$  and  $\Delta H_{\text{water}}^{\text{AB}}$  did not show good correlation at 65% relative humidity, which suggests a change in the nature of the surface interactions of the water vapor with the wood particles. A surprising aspect of these results was the slight increase in the correlation between  $\Delta W\%$  and  $K_A$  at 65% relative humidity. Although this result raises an interesting question about how the surface Lewis acid-base characteristics of the wood particles influence the adsorption of water vapor beyond monolayer coverage, it appears

**Table II** Surface Acid-Base Enthalpy of Desorption ( $\Delta H^{\text{AB}}$ ) of Acid-Base Probes on Wood Particles<sup>a</sup>

Probe	$\Delta H^{\text{AB}}$ (kJ/mol) on Various Types of Particles		
	Unwashed	Washed	Treated
$\text{CCl}_4$	-1	-1	-1
$\text{CHCl}_3$	4	6	8
$\text{C}_2\text{H}_5\text{OC}_2\text{H}_5$	1	16	10
$\text{CH}_3\text{COOC}_2\text{H}_5$	9	24	21

<sup>a</sup> Derived from slopes of regression lines in Figures 2-4.

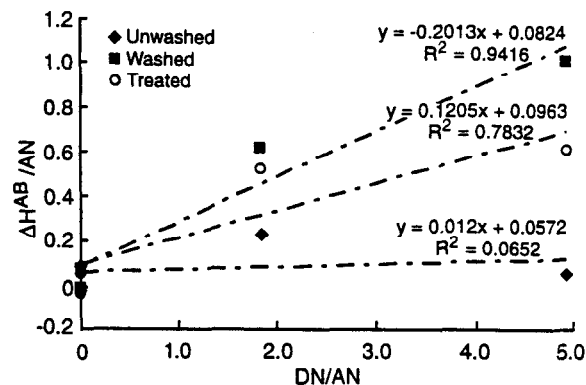


**Figure 7**  $\Delta H^{\text{AB}}/AN$  versus  $DN/AN$  for unwashed, washed, and treated wood particles.

to be consistent with the evolution of a multilayer hydrated surface whose structure is dependent upon the magnitude of  $K_A$ . Thus, it can be argued that the key to controlling the water vapor adsorption behavior of wood particles lies in the ability to manipulate the surface acid-base enthalpy of interaction of the wood particles with water. The strong correlation between  $\Delta W\%$  and  $K_A$  implies that, of the two possible pathways for manipulating the magnitude of  $\Delta H_{\text{water}}^{\text{AB}}$  via the surface acceptor-donor parameters, the greatest effect may be achieved by surface modification reactions that result in a decrease of the magnitude of  $K_A$ . A typical example of manipulating  $K_A$  is the substitution of the hydrogen acceptor sites on the hydroxyl groups with an alkyl group as proposed in Figure 3(B). Note, however, that water has a relatively high acceptor number and, therefore, the capacity to interact with surfaces that have very low donor parameters. Thus: surface modification reactions that also limit the accessibility of the surface donor sites to the acceptor site of water are also important. Such reactions may be regarded as  $K_D$ -controlling reactions. An example of the latter would be the steric hindrance of the oxygen donor by means of

**Table III** Surface Acceptor and Donor Parameters for Wood Particles

Particles (Dimensionless)	$K_A$	$K_D$ (kcal/mol)	$\Delta H_{\text{water}}^{\text{AB}}$ (kJ/mol) <sup>a</sup>
Unwashed	$0.012 \pm 0.03$	$0.057 \pm 0.08$	14
Washed	$0.20 \pm 0.04$	$0.082 \pm 0.09$	33
Treated	$0.12 \pm 0.05$	$0.096 \pm 0.12$	31

<sup>a</sup> Calculated according to eq. (5).

**Table IV XPS Analysis of Surface Chemical Composition of Wood Particles**

Particles	Peak Intensity Relative to Total Area of C1s Peak					
	O <sup>a</sup>	C—C; C—H	C—O; C—O—C	O—C=O	O—C(—O)=O	C—Si
Unwashed	0.28	0.77	0.14	0.093	0	0
Washed	0.47	0.68	0.17	0.120	0	0
Treated	0.45	0.44	0.40	0.081	0.028	0.048

<sup>a</sup> Total area of O1s peak.

a bulky substituent on the hydroxyl group, such as a trialkyl-silyl group [see Fig. 3(A)].

### Dispersive Component of Surface Energy

The dispersive components of the surface energy of the wood particles are summarized in Table VI and plotted as a function of temperature in Figure 8. Extrapolated values of  $\gamma_S^D$  at 27°C were calculated from the linear regression equations of the plots of  $\gamma_S^D$  as a function of temperature and tested for correlation with  $\Delta W\%$ . Although water has a permanent dipole that is capable of relatively strong dispersive interactions with the surface molecules of wood particles, there was poor correlation between  $\Delta W\%$  and  $\gamma_S^D$  at 30% relative humidity (Table V). However, the correlation improved at 65% relative humidity, indicating a change in the nature of the surface interactions of wood with the water vapor.

### CONCLUSIONS

The percentage of weight gain of wood particles exposed to relative humidity of 30 or 65% and a dry-bulb temperature of 27°C showed strong correlation with the value of the surface acid-base enthalpy of interaction with water, calculated

**Table V Correlation of  $\Delta W\%$  with  $\Delta H_{\text{water}}^{\text{AB}}$ ,  $K_A$ ,  $K_D$ , and  $\gamma_S^D$** 

	$\Delta W\%$	
	30% RH	65% RH
	$\Delta W\%$	1
$\Delta H_{\text{water}}^{\text{AB}}$	0.9798	0.9175
$K_A$	0.9867	0.9990
$K_D$	0.7019	0.5399
$\gamma_S^D$	0.8128	0.9154

from the surface acceptor and donor parameters determined from IGC measurements. This strong correlation suggests two possible pathways for manipulating the magnitude of the surface acid-base enthalpy of interaction with water vapor. For amphoteric substrates, with a relatively stronger tendency to accept electrons, the magnitude of the acid-base enthalpy of interaction with water vapor may be controlled via the acceptor parameter,  $K_A$ . Practical examples of achieving this control are substituting the hydrogens in the hydroxyl groups with neutral groups such as an alkyl or alkyd-silyl group, or limiting accessibility to the oxygen atoms by steric hindrance with bulky substituents such as a trialkylsilane on the hydroxyl group (see Fig. 3). The relationship between the surface functional groups and the magnitude of  $\Delta H_{\text{water}}^{\text{AB}}$  remains ambiguous and merits further study. The mechanism of the influence of  $K_A$  on the adsorption of multilayers of water vapor also merits further study.

The Forest Products Laboratory is maintained in cooperation with the University of Wisconsin. **This** article was

**Table VI Dispersive Component of Surface Energy of Wood Particles at Different Temperatures**

Temperature (°C)	$\gamma_S^D$ (mJ/m <sup>2</sup> )		
	Unwashed Particles	Washed Particles	Treated Particles
27	41 <sup>a</sup>	53 <sup>a</sup>	43 <sup>a</sup>
40	38	50	42
50	37	46	38
60	33	43	34
80	33	39	27
100	24	31	30

<sup>a</sup> Extrapolated values calculated from linear regression equations for  $\gamma_S^D$  versus temperature.



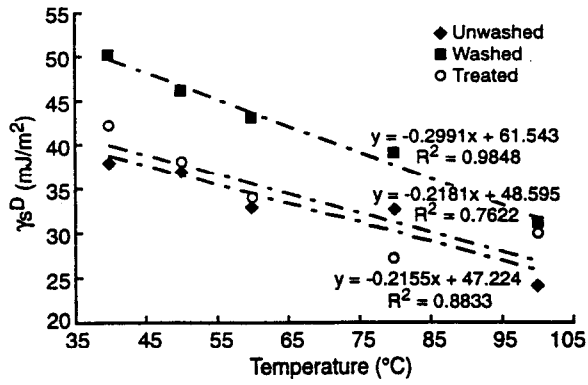


**Figure 8**  $\gamma_s^D$  as a function of temperature for unwashed, washed, and treated wood particles.

written and prepared by U.S. Government employees on official time, and it is, therefore, in the public domain and not subject to copyright. We gratefully acknowledge the USDA Forest Service, Forest Products Laboratory, for providing financial support for this project.

## REFERENCES

- Sanadi, A. R.; Caulfield, D. F.; Jacobson, R. E.; Rowell, R. M. *I&EC Res* 1995, 34, 1889.
- Marcovich, N. E.; Reboledo, M. M.; Aranguren, M. I. *J Appl Polym Sci* 1996, 61, 119.
- Chtourou, H.; Riedl, B.; Kokta, B. V. *J Adhes Sci Technol* 1995, 9, 551.
- Sain, M. M.; Kokta, B. V.; Maldas, D. *J Adhes Sci Technol* 1993, 7, 49.
- Joly, C.; Gauthier, R.; Escoubes, M. *J Appl Polym Sci* 1996, 61, 57.
- Fowkes, F. M. *J Adhes Sci Technol* 1987, 1, 7.
- Gutmann, V. *The Donor-Acceptor Approach to Molecular Interactions*; Plenum Press: New York, 1978.
- Riddle, F. L., Jr.; Fowkes, F. M. *J Am Chem Soc* 1990, 112, 3259.
- Fowkes, F. M. *J Adhes Sci Technol* 1990, 4, 669.
- Schultz, J.; Lavielle, L.; Martin, C. *J Adhes* 1987, 23, 45.
- Saint Flour, C.; Papirer, E. *Ind Eng Chem Prod Res Dev* 1982, 21, 666.
- Avramidis, S.; Dubois, J. *Holzforschung* 1992, 46, 177.
- Nguyen, T.; Johns, W. E. *Wood Sci Technol* 1978, 12, 63.
- Berg, J. C. *Nordic Pulp Paper Res J* 1993, 1, 75.
- Kamdem, D. P.; Bose, S. K.; Luner, P. *Langmuir* 1993, 9, 3039.
- Tshabalala, M. A. *J Appl Polym Sci* 1997, 65, 1013.
- Billo, e. J. *Excel® for Chemists. A Comprehensive Guide*; Wiley-VCH: New York, 1997.
- Cai, S.; Fang, J.; Yu, X. *J Appl Polym Sci* 1992, 44, 135.
- Tajima, I.; Yamamoto, M. *J Polym Sci Chem Ed* 1985, 23, 615.
- Samadi, M.; Denes, F. *TAPPI J* 1996, 79, 189.